

## Kinetic and thermodynamic studies of the removal of murexide from aqueous solutions on to activated carbon

Ardeshir Shokrollahi<sup>\*</sup>, Mehrourang Ghaedi, Mojdeh Ranjbar, Ameneh Alizadeh

*Department of Chemistry, University Yasouj, 75918-74831, Yasouj, Iran*

Received 10 November 2010; received in revised form 30 November 2010; accepted 30 November 2010

### Abstract

The objective of this study was to assess the adsorption potential of activated carbon (AC) as an adsorbent for the removal of Murexide (Mu) from aqueous solutions. The influence of variables parameters including pH, amount of adsorbent, sieve size of adsorbent, temperature and contact time on Mu removal was studied. Following optimization of variables, the relation between concentrations of dye remained in aqueous and adsorbent has been evaluated using various adsorption isotherm models like, Langmuir, Freundlich, Tempkin, Harkins-Jura and Dubinin–Radushkevich. Thermodynamic parameters such as enthalpy ( $\Delta H^\circ$ ), and, entropy ( $\Delta S^\circ$ ), activation energy ( $E_a$ ), sticking probability ( $S^*$ ), and Gibb's free energy changes ( $\Delta G^\circ$ ) were also calculated. It was found from evaluated different thermodynamic parameters, viz.,  $\Delta H^\circ$ ,  $\Delta S^\circ$  and  $\Delta G^\circ$  that the adsorption of Mu by AC was feasible, spontaneous and endothermic process. The kinetic studies suggest that the all process following pseudo second order kinetics and involvement of inter- particle diffusion mechanism. The results indicated that the intraparticle diffusion also is the rate limiting factor.

**Keywords:** Adsorption; Murexide; Activated carbon; Adsorption isotherm; Thermodynamics; Kinetic of adsorption.

### 1. Introduction

Most dyes are considered to be non-oxidizable substances by conventional biological and physical treatment because of their complex structure and large molecular size. The adsorption process provides an attractive alternative treatment, especially if the adsorbent is inexpensive and readily available. Granular activated carbon is the most popular adsorbent and has been used with great success.

High volumes of aqueous effluents contaminated with dyes are generated by different industries. The removal of dyes from aquatic environment, is extremely important from the healthiness point of view because most of these dyes are toxic, causing allergy, skin irritation, besides most of them are Mutagenic and/or carcinogenic [1–3]. Therefore, industrial effluents containing dyes need to be treated before being delivered to environment [4, 5]. Treatment of the effluent from the dyeing and finishing processes in the textile industry is one of the most significant environmental problems. Since most synthetic dyes have complex aromatic molecular structures which make them inert and biodegradable difficult when discharged into the

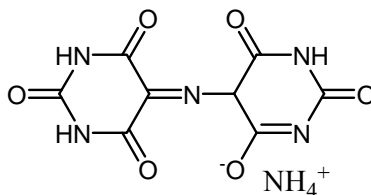
<sup>\*</sup> Corresponding author. Tel. +98 741 2223048.  
E-mail address: ashokrollahi@mail.yu.ac.ir (A. Shokrollahi)

environment. Colored wastes are harmful to aquatic life in rivers, lakes and Sea where they are discharged [6-8].

The Murexide (Mu) is an organic compound applied as a complexometric indicator for complexometric titration of the alkali metal ions in some non-aqueous solutions [9]. It investigated as promising enhancer of sonochemical destruction of chlorinated hydrocarbon pollutants. The dye color changes are probably due to the displacement of protons from the imido groups; since there are four such groups [10].

The methods of color removal from industrial effluents include biological treatment, coagulation, flotation, adsorption, oxidation and hyperfiltration [11, 12]. Among the treatment options, adsorption has been found to be superior to other techniques for water treatment in terms of initial cost, simplicity of design, ease of operation and insensitivity of toxic substances. Subsequently, the adsorbent can be regenerated or kept in a dry place without direct contact with the environment [13].

Different adsorbents have been used for the removal from aqueous solutions of various materials, such as dyes, metal ions and other organic materials includes perlite [14–19], bentonite [20], silica gels [21], fly ash [22], lignite [23], peat [24], silica [25], etc. AC is the most employed adsorbent for Mu removal from aqueous solution because of its excellent adsorption properties. The high adsorption capacity of an AC is associated with its high surface area and porous structure. Besides these physical characteristics, the adsorption capacity is also dependent from source of the organic material employed or the production of the AC, as well as the experimental conditions employed in the activation processes [26-28]. In continuous to the attempt of other researches by using AC, the work is in progress to applied the AC and evaluate it capability to removal Mu from water. The chemical structure of Mu is illustrated in Scheme1.



**Scheme 1.** Chemical structure of Mu.

## 2. Experimental

### 2.1. Instruments and Reagents

Stock solution was prepared by dissolving require amount of Mu in double distilled water. Aqueous solutions of Mu are unstable and must be prepared each day. The test solutions were prepared by diluting stock solution to the desired concentrations. The concentration of the Mu was determined at 256 nm. The pH measurements were done using pH/Ion meter model-686 and adsorption studies were carried out on Jasco model V-570 spectrophotometer (Jasco Co., Hachioji, Tokiyo, Japan). All chemicals include NaOH, HCl, KCl, Activated carbon (AC) (analytical-grade, 40-50 mesh from Merck) and Mu with the highest purity available are purchased from Merck, Darmstadt, Germany.

### 2.2. Measurements of Mu adsorption

To study the effect of important parameters like the pH, adsorbent dosage, contact time, initial dye concentration and temperature on the adsorptive removal of Mu batch experiments were conducted. For each experimental run, 50 mL of Mu solution of known concentration, pH and amount of the adsorbent were taken in a 100 mL Erlenmeyer flask with middle magnet. This mixture was agitated on stirrer at a constant speed in a temperature controlled. Samples were withdrawn at different time intervals (0–10 min for AC) and kinetics, thermodynamic, isotherm

and other parameters of adsorption was determined by analyzing of remaining dye concentration from aqueous solution.

Experiments were carried out at pH=1.0 that the initial pH of the solution was adjusted by addition of aqueous solutions of HCl or NaOH. The percentage removal of dye was calculated using the following relationship:

$$\% \text{ Mu removal} = ((C_0 - C_t)/C_0) \times 100 \quad (1)$$

where  $C_0$  (mg/L) and  $C_t$  (mg/L) are the initial dye concentration and dye concentration at time  $t$ , respectively.

For adsorption isotherms, dye solutions of different concentrations (25-200 mg/L) and at different temperatures (10–60 °C) were agitated with known amounts of adsorbents until the equilibrium was achieved. Equilibrium adsorption capacity was calculated from the relationship:

$$q_e = \frac{(C_0 - C_e).V}{W} \quad (2)$$

where  $C_0$  and  $C_e$  are the initial and equilibrium dye concentrations in solution, respectively (mg/L),  $V$  the volume of the solution (L) and  $W$  is the mass (g) of the adsorbent used [29].

### 3. Results and discussion

#### 3.1. Effect of particle size

The particle size distribution of AC determined by sieving the samples manually shaking with stainless steel mesh screens of standard (international ASTM with meshes 10, 20, 30, 40 and 50). For batch adsorption experiments, three different particle sizes viz. 10-20, 20-30 and 40-50 AC mesh were selected and difference in the amount adsorbed was noticed by using different mesh sizes. Effect of sieve size of adsorbent on the adsorption was studied at  $30 \pm 0.5$  °C, 0.4 g of AC, pH=1.0 and Mu concentration of 100 mg/L. Table 1 presents effect of sieve size of adsorbent on the adsorption at  $30 \pm 0.5$  °C. It was observed that adsorption was found to increase with the 40-50 mesh sizes. This is due to increase in the surface area of the adsorbent and accessibility of the adsorbent pores towards the Mu [30].

**Table 1**

Effect of different sieve sizes.

Mesh size	Amount absorbed (mg/g)
10-20	11.1
20-30	11.3
40-50	11.6

#### 3.2. Effect of pH on Mu adsorption

Solution pH affects both aqueous chemistry and surface binding sites of the adsorbents. The effect of initial pH on adsorption of Mu was studied from pH 1.0 to 5.0 at  $30 \pm 0.5$  °C temperature, at initial Mu concentration of 100 mg/L, adsorbent dosage of 0.4 g and contact time of 6 min. The maximum adsorption of the Mu is obtained at pH =1.0. Fig. 1. depicts that the pH significantly affects the extent of adsorption of dye over the adsorbent and a maximum in the amount adsorbed with decreasing pH was observed. The acidity constant value of the most acidic group of the Mu molecule is 1.6. This functional group can be easily dissociated and thus, the Mu molecule has net negative charges in the working experimental conditions. [31-33].

Two possible mechanism of adsorption of Mu on the AC adsorbent may be considered: (a) electrostatic interaction between the adsorbent and the Mu molecule, (b) a chemical reaction between the Mu and the adsorbent. At acidic pH the  $H^+$  ion concentration in the system increased and the surface of the AC acquires positive charge by absorbing  $H^+$  ions. As the pH of the system increases, the number of negatively charged sites increases and the number of positively charged sites decreases. Negatively charged surface sites on the AC do not favor the adsorption of Mu anions due to the electrostatic repulsion. Also lower adsorption of Mu at alkaline pH is due to the presence of excess  $OH^-$  ions, which destabilize anionic Mu and compete with the Mu anions for the adsorption sites. The most effective pH was 1.0 and it was used in further studies [34, 35].

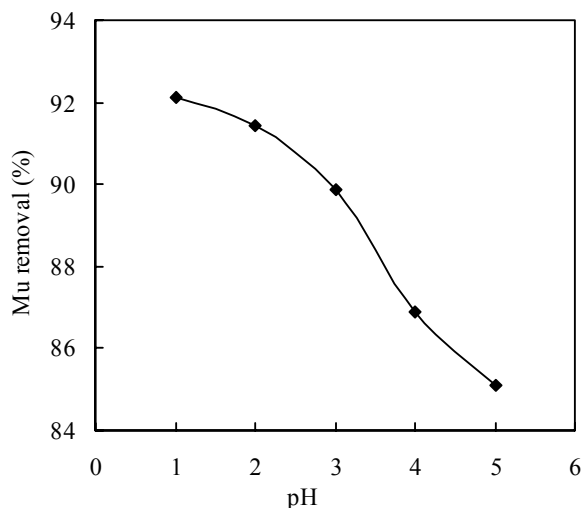


**Fig. 1.** Effect of pH on adsorption of Mu (100 mg/L) onto AC (0.4 g/50 mL) at temperature  $30 \pm 0.5$  °C.

### 3.3. Adsorbent dosage

The study of adsorbent dosages for removal of the Mu from aqueous solution was carried-out using mass of AC adsorbent ranging from 0.05 to 0.6 g and fixing the initial Mu concentration at 100 mg/L. It was observed that highest amount of Mu removal was attained for adsorbent mass of at least adsorbent (Fig. 2).

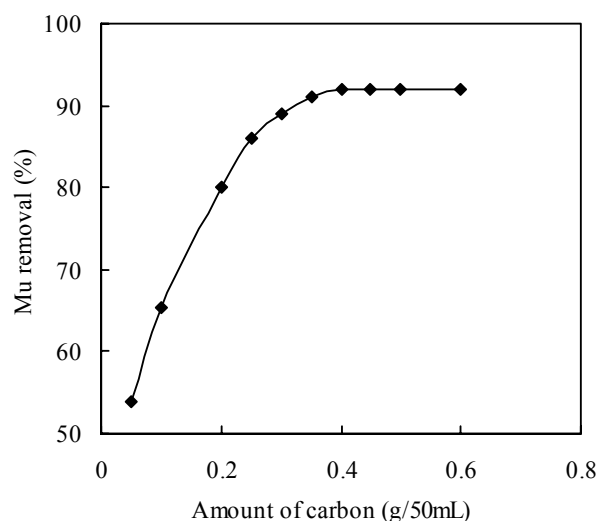


**Fig. 2.** Effect of AC amount on Mu removal,  $C_0 = 100$  mg/L at pH= 1.0, agitation speed: 400 rpm and temperature  $30 \pm 0.5$  °C.

For adsorbent masses higher than 0.4 g for 100 mg/L the Mu removal remained almost constant. Increases in the percentage of Mu removal with adsorbent masses could be attributed to increases in the adsorbent surface areas, augmenting its number of adsorption sites available for adsorption, as already reported in several papers [36, 37]. It should be stressed that the addition of increasing masses (0.05–0.6 g) of AC added to the Mu solution (pH=1.0) did not promoted remarkable changes at the initial pH of the Mu solution. In order to continue this work, the adsorbent masses were fixed at 0.4 g at 100 mg L<sup>-1</sup>, since these adsorbent asses correspond to the minimum amount of adsorbent which lead to a constant and maximum removal of Mu.

### 3.4. Effect of contact time on Mu removal

The adsorption rate, obtained for Mu adsorption on AC was observed by decrease of the concentration of Mu within the adsorption medium with contact time. The time necessary to reach equilibrium for the removal of the Mu molecules at three concentration of 50, 100 and 200 (mg/L) by AC from aqueous solution was established about 6 minutes. After equilibrium, the amount of adsorbed dye did not change significantly with time in Fig. 3.

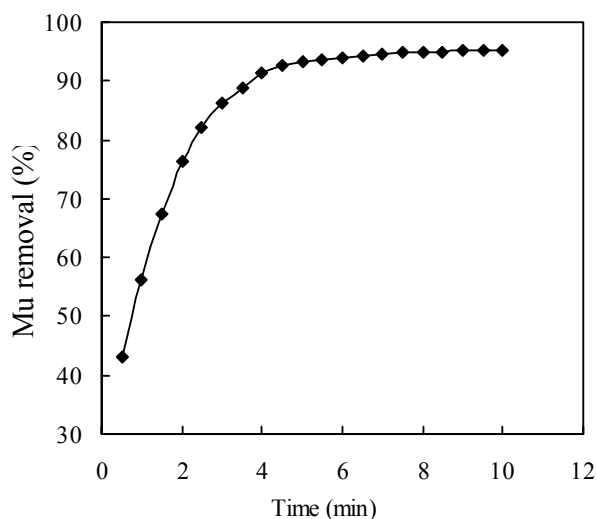


**Fig. 3.** Effect of contact time on the removal of Mu with initial concentration 100 mg/L at temperature  $30 \pm 0.5$  °C on optimum condition: AC amount 0.4 g/50mL, agitation speed 400 rpm, contact time 6 minutes and pH=1.0.

At 100 mg/L of Mu, the removal rate in the first varies from 31.4% to 92.3% of the maximum removal onto AC. For instance, the adsorbents exhibited three stages, which can be attributed to each linear portion of the figure. The first linear portion was attributed to the diffusion process of Mu to the adsorbent surfaces [38, 39], hence, was the fastest adsorption stage. This result is corroborated by the factionary-order kinetic model. The second linear portion was attributed to intra-particle diffusion, which was delayed process. The third stage may be regarded as the diffusion through smaller pores, which is followed by the establishment of equilibrium [38, 39]. The surface of AC may contain a large number of active sites and the solute adsorption can be related to the active sites on equilibrium time. Also up to 90–92.3% of the total amount of Mu adsorption was found to occur in the first rapid phase (10 min) and thereafter the adsorption rate was found to decrease. The higher adsorption rate at the initial period (first 6 min) may be due to too number of vacant sites available at the initial stage. As a result there exist too concentration gradients between adsorbate in solution and onto adsorbent surface. This increased in concentration gradients tends to increase in Mu adsorption at the initial stages.

### 3.5. Adsorption kinetics study

Kinetic models are used to examine the rate of the adsorption process and potential rate-controlling step. The adsorption rate is strongly influenced by several parameters related to the state of the solid, generally having very heterogeneous reactive surface, and to the physicochemical conditions under which adsorption is carried out. In order to investigate the adsorption processes of Mu on the adsorbent, pseudo-first-order, pseudo-second-order, Elovich and intra-particle diffusion kinetic models were studied.

#### 3.5.1. Pseudo-first-order model

The pseudo-first-order model was described by Lagergren [40]

$$\frac{dq_t}{q_t} = K_1(q_e - q_t) \quad (3)$$

where  $q_e$  and  $q_t$  refer to the amount of dye adsorbed ( $\text{mg g}^{-1}$ ) at equilibrium and at any time,  $t$  (min), respectively and  $K_1$  is the equilibrium rate constant of pseudo-first-order adsorption ( $\text{min}^{-1}$ ). Integration of Eq. (2) for the boundary conditions  $t = 0$  to  $t$  and  $q_t = 0$  to  $q$  gives:

$$\text{Log}(q_e - q_t) = \text{Log}q_e - \frac{K_1}{2.303} \cdot t \quad (4)$$

The values of  $\log(q_e - q_t)$  were linearly correlated with  $t$ . The plot of  $\log(q_e - q_t)$  vs.  $t$  should give a linear relationship from which the values of  $K_1$  were determined from the slope of the plot (Table 2). In many cases, the first-order equation of Lagergren does not fit well with the whole range of contact time and is generally applicable over the initial stage of the adsorption processes (Fig. 4) [41]. The calculated  $q_e$  values are not close to the experimental  $q_e$  values which indicate that the adsorption of Mu onto Ac is not a first order reaction.

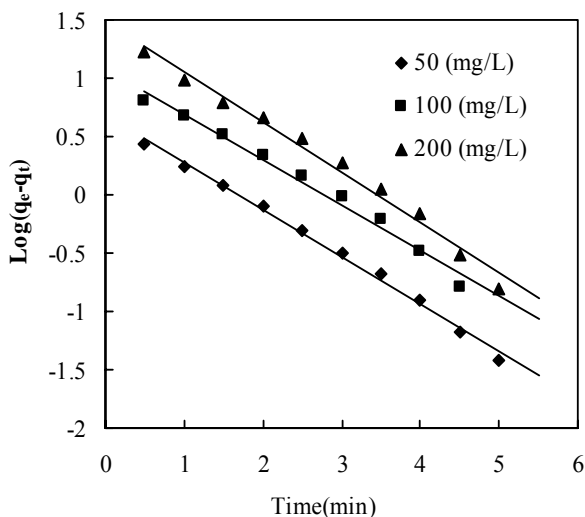


**Fig. 4.** Pseudo-first-order kinetic model plot for the adsorption of Mu with concentrations 50, 100 and 200 mg/L, at temperature  $30 \pm 0.5$  °C on optimum condition: AC amount 0.4 g/50 mL, agitation speed 400 rpm, contact time 6 min and pH=1.0.

**Table 2**

Adsorption kinetic parameters for the adsorption of Mu at temperature  $30 \pm 0.5$  °C on condition optimum: AC amount 0.4 g/50 mL, agitation speed 400 rpm, contact time 6 min and pH=1.0.

Model	parameters	Initial Mu concentration (mg/L)		
		50	100	200
First-order kinetic	$k_1$	0.91	0.89	0.91
	$q_e$ (calc)	1.92	12.82	31.02
	$R^2$	0.99	0.98	0.98
Second-order kinetic	$k_2$	0.37	0.13	0.62
	$q_e$ (calc)	6.16	12.08	25.91
	$R^2$	1.00	0.99	1.00
	$h$	14.14	20.41	41.32
Intraparticle diffusion	$K_{diff}$	0.17	0.31	0.71
	$C$	5.34	10.96	21.93
	$R^2$	0.86	0.94	0.96
Elovich	$\beta$	1.14	0.46	0.19
	$\alpha$	2.38	5.85	13.87
	$R^2$	0.90	0.91	0.87
$q_e$ (exp)		5.77	11.73	23.65

### 3.5.2. Pseudo-second-order model

The pseudo-second-order model [42] is represented by the following differential equation

$$\frac{dq_t}{dt} = K_2(q_e - q_t)^2 \quad (5)$$

where  $K_2$  is the equilibrium rate constant of pseudo-second-order adsorption ( $\text{g mg}^{-1} \text{min}^{-1}$ ). Integrating Eq. (4) for the boundary condition  $t = 0$  to  $t$  and  $q_t = 0$  to  $q_t$ , gives:

$$\frac{t}{q_t} = \frac{1}{K_2 \cdot q_e^2} + \frac{1}{q_e} t \quad (6)$$

The slope and intercept of plot of  $t/q_t$  vs.  $t$  were used to calculate the second-order rate constant  $K_2$  (Fig. 5). The values of equilibrium rate constant ( $K_2$ ) are presented in Table 2. The

correlation coefficients of all examined data were found very high ( $R^2 \geq 0.99$  and 1.00) and calculated  $q_e$  are almost near experimental  $q_e$  values, This shows that the model can be applied for the entire adsorption process and confirms that the adsorption of Mu dye on AC follows the pseudo-second-order kinetic model.

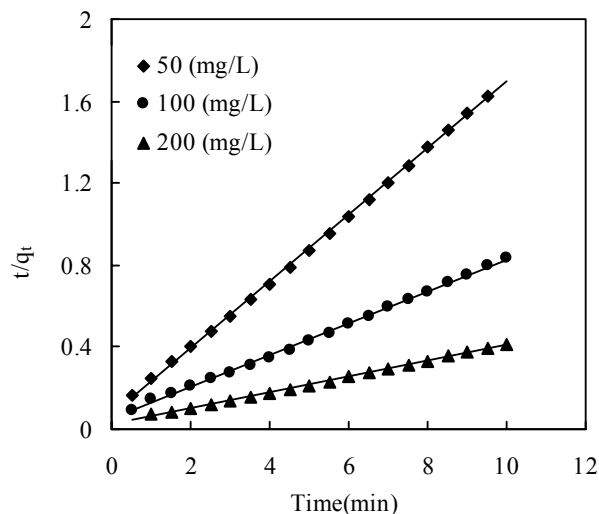


**Fig. 5.** Pseudo-second-order kinetic model plot for the adsorption of Mu with concentrations 50, 100 and 200 mg/L, at temperature  $30 \pm 0.5$  °C on optimum condition: AC amount 0.4 g/50 mL, agitation speed 400 rpm, contact time 6 min and pH=1.0.

### 3.5.3. Elovich kinetic equation

The Elovich equation is another rate equation based on the adsorption capacity is given as follows [43]:

$$\frac{dq_t}{dt} = \alpha \exp(-\beta q_t) \quad (7)$$

where  $\alpha$  is the initial adsorption rate ( $\text{mg g}^{-1} \text{min}^{-1}$ ) and  $\beta$  is the de-sorption constant ( $\text{gmg}^{-1}$ ) during any one experiment. It is simplified by assuming  $\alpha \beta \gg t$  and by applying the boundary conditions  $q_t = 0$  at  $t = 0$  and  $q_t = q_t$  at  $t = t$  Eq. (7) rewrite as followed:

$$q_t = \frac{1}{\beta} \ln(\alpha\beta) + \frac{1}{\beta} \ln(t) \quad (8)$$

Plot of  $q_t$  versus  $\ln(t)$  should yield a linear relationship if the Elovich is applicable with a slope of  $(1/\beta)$  and an intercept of  $(1/\beta) \ln(\alpha\beta)$  (Fig. 6). The Elovich constants obtained from the slope and the intercept of the straight line reported in Table 2. The correlation coefficients  $R^2$  are very wavy and ranged from low value to high value without definite role (Table 2).

### 3.5.4. Intra-particle diffusion model

The adsorption mechanism of adsorbate onto adsorbent follows three steps: film diffusion, pore diffusion and intra-particle transport. The slowest of three steps controls the overall rate of the process. Generally, intra-particle diffusion is often rate-limiting in a batch reactor, while for a continuous flow system film diffusion is more likely the rate-limiting step. In order to investigate

the possibility of intra-particle diffusion resistance affecting the adsorption intra-particle diffusion model [44] was explored.

$$q_t = K_{dif} t^{0.5} + C \quad (9)$$

where  $K_{dif}$  is the intra-particle diffusion rate constant. Fig. 7 represents a plot of  $q_t$  vs.  $t^{0.5}$  for all adsorbents. It shows two separate regions, the initial part is attributed to the bulk diffusion while the final part to the intra-particle diffusion. Values of  $C$  give an idea about the thickness of boundary layer (Table 2), i.e. the larger the intercept the greater is the boundary layer effect. The data indicate that intra-particle diffusion controls the adsorption rate. Simultaneously, external mass transfer resistance cannot be neglected although this resistance is only significant for the initial period of time [45].

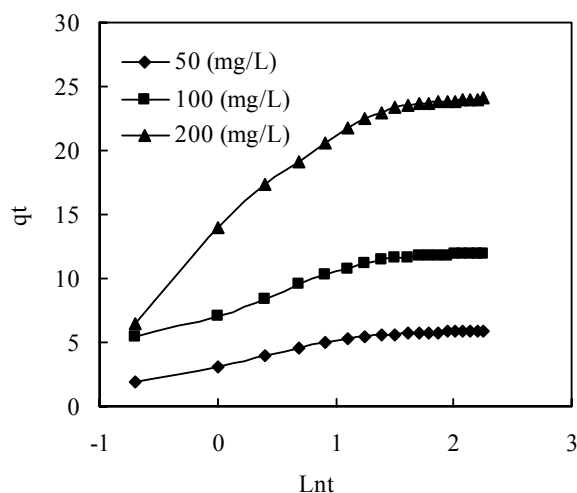


**Fig. 6.** Elovich kinetic model plot for the adsorption of Mu with concentrations 50, 100 and 200 mg/L, at temperature  $30 \pm 0.5$  °C on optimum condition: AC amount 0.4 g/50 mL, agitation speed 400 rpm, contact time 6 min and pH=1.0.

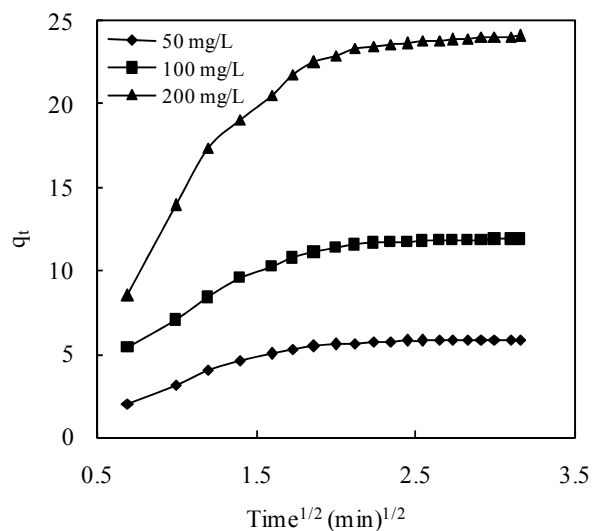


**Fig. 7.** Intraparticle diffusion model plot for the adsorption of Mu with concentrations 50, 100 and 200 mg/L, at temperature  $30 \pm 0.5$  °C on optimum condition: AC amount 0.4 g/50 mL, agitation speed 400 rpm, contact time 6 min and pH=1.0.

### 3.6. Adsorption equilibrium study

Adsorption isotherms are prerequisites to understand the nature of the interaction between adsorbate and the adsorbent used for the removal of organic pollutants. An adsorption isotherm describes the relationship between the amount of adsorbate up taken by the adsorbent and the adsorbate concentration remaining in solution [46, 47]. There are many equations for analyzing experimental adsorption equilibrium data. The equation parameters of these equilibrium models often provide some insight into the adsorption mechanism, the surface properties and affinity of the adsorbent for adsorbate [47- 49].

The parameters obtained from the different models provide important information on the surface properties of the adsorbent and its affinity to the adsorbate. Several isotherm equations have been developed and employed for such analysis and the three important isotherms, the Langmuir, Freundlich, Tempkin, Dubinin-radushkevich and Harkins-Jura isotherms are applied in this study. The Langmuir isotherm is based on the assumption that the adsorption process takes place at specific homogeneous sites within the adsorbent surface and that once a dye molecule occupies a site, no further adsorption can take place at that site, which concluded that the adsorption process is monolayer in nature.

The Langmuir equation, which is valid for monolayer adsorption onto a completely homogenous surface with a finite number of identical sites with negligible interaction between adsorbed molecules, is represented in the linear form as follows: [47]

$$\frac{1}{q_e} = \left(\frac{1}{K_L Q_m}\right) \cdot \left(\frac{1}{C_e}\right) + \frac{1}{Q_m} \quad (10)$$

where  $K_L$  is the Langmuir adsorption constant (L/mg) and  $Q_m$  is the theoretical maximum adsorption capacity (mg/g). Figure 8 shows the Langmuir ( $C_e/q_e$  vs.  $C_e$ ) plots for adsorption of Mu at  $30 \pm 0.5$  °C temperature. The value of  $Q_m$  and  $K_L$  constants and the correlation coefficients for Langmuir isotherm are presented in Table 3. The isotherms of Mu on AC was found to be linear over the whole concentration range studies and the correlation coefficients were extremely high ( $R^2 > 0.97$ ) as shown in Table 3.

The Freundlich isotherm [50] is derived by assuming a heterogeneous surface with a non-uniform distribution of adsorption heat over the surface was presented in the linear form as follows:

$$\text{Log}q_e = \text{Log}K_f + \left(\frac{1}{n}\right)\text{Log}C_e \quad (11)$$

where  $K_f$  (L/mg) and  $n$  is isotherm constants indicate the capacity and intensity of the adsorption, respectively. The  $1/n$  factor also indicate heterogeneity factor. Figure 8 shows the Freundlich ( $\log q_e$  vs.  $\log C_e$ ) plots for adsorption of Mu at  $30 \pm 0.5$  °C temperatures. Table 3 shows the Freundlich adsorption isotherm constant and its respective correlation coefficients.

Heat of adsorption and the adsorbent–adsorbate interaction on adsorption isotherms were studied by Tempkin [51] and its equation is given as:

$$q_e = \frac{RT}{b} \text{Ln}(K_T C_e) \quad (12)$$

Eq. (12) can be linearized as:

$$q_e = B_T \text{Ln}K_T + B_T \text{Ln}C_e \quad (13)$$

where  $B_T = RT/b_T$ ,  $T$  is the absolute temperature in K,  $R$  the universal gas constant,  $8.314 \text{ J mol}^{-1} \text{ K}^{-1}$ ,  $K_T$  the equilibrium binding constant (L/mg) and  $B_T$  is related to the heat of adsorption.

**Table 3**

Comparison of the coefficients isotherm parameters for Mu adsorption onto AC.

Isotherm models	Parameters	Temperature		
		303.15	313.15	
<i>Langmuir</i> $\frac{1}{q_e} = \left(\frac{1}{K_1 Q_m}\right) \cdot \left(\frac{1}{C_e}\right) + \frac{1}{Q_m}$	$K_1$ (L/mg)	0.053	0.051	
	$Q_m$ (mg/g)	12.88	16.78	
	$R^2$	0.91	0.97	
	$\chi^2 = \sum_{i=1}^m \left(\frac{q_{e,\text{exp}} - q_{e,\text{calc}}}{q_{e,\text{exp}}}\right)^2$	$R_L$	0.16	0.16
		$\chi^2$	0.87	0.66
<i>Freundlich</i> $\text{Log}q_e = \text{Log}K_f + \left(\frac{1}{n}\right)\text{Log}C_e$	$1/n_f$	1.43	0.77	
	$K_f$ (L/mg)	0.54	3.69	
	$R^2$	0.94	0.96	
	$\chi^2 = \sum_{i=1}^m \left(\frac{q_{e,\text{exp}} - q_{e,\text{calc}}}{q_{e,\text{exp}}}\right)^2$	$\chi^2$	1.82	1.36
<i>Tempkin</i> $q_e = B_T \text{Ln}K_T + B_T \text{Ln}C_e$	$K_T$ (L/mg)	0.31	1.36	
	$B_T$	14.19	7.69	
	$bt$	177.62	338.29	
	$R^2$	0.97	0.91	
	$\chi^2 = \sum_{i=1}^m \left(\frac{q_{e,\text{exp}} - q_{e,\text{calc}}}{q_{e,\text{exp}}}\right)^2$	$\chi^2$	0.15	0.16
<i>Dubinin-Radushkevich</i> $\text{Ln}q_e = \text{Ln}Q_m - k\varepsilon^2$	$Q_m$ (mg/g)	23.07	14.86	
	$K \times 10^{-7}$	0.6	6	
	$E$ (Kj/mol)	288.67	917.43	
	$R^2$	0.95	0.92	
	$\chi^2 = \sum_{i=1}^m \left(\frac{q_{e,\text{exp}} - q_{e,\text{calc}}}{q_{e,\text{exp}}}\right)^2$	$\chi^2$	1.41	2.58
<i>Harkins-Jura</i> $\frac{1}{q_e} = \left(\frac{B_2}{A}\right) - \left(\frac{1}{A}\right)\text{Log}C_e$	$A$	5.89	12.59	
	$B_2$	1.07	0.93	
	$R^2$	0.62	0.66	
	$\chi^2 = \sum_{i=1}^m \left(\frac{q_{e,\text{exp}} - q_{e,\text{calc}}}{q_{e,\text{exp}}}\right)^2$	$\chi^2$	8.63	9.57

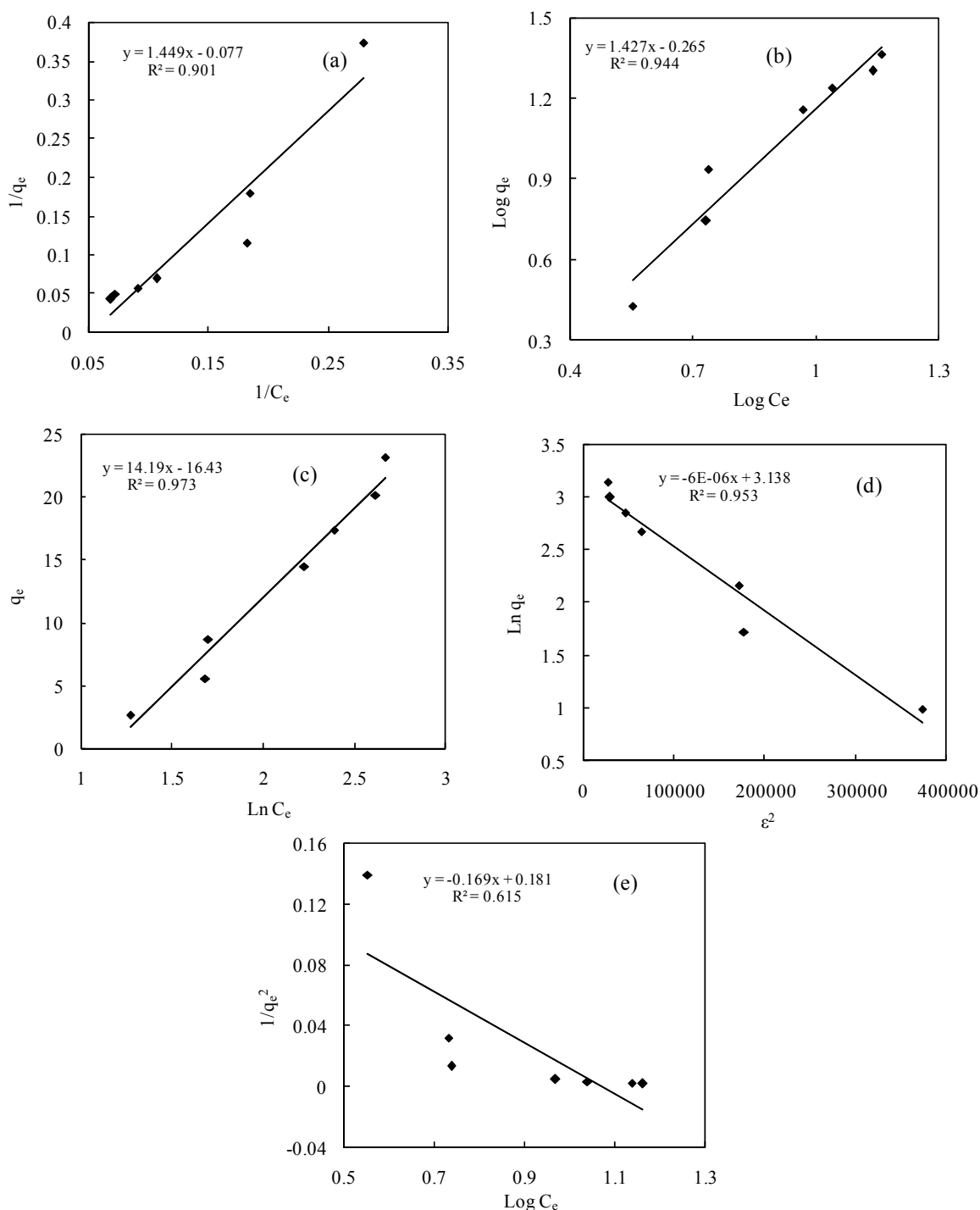


**Fig. 8.** Langmuir (a), Freundlich (b), Tempkin (c), Dubinin- Radushkevich (d) and Harkins-jura (e) isotherm models plot for the adsorption of Mu with concentrations 50, 100 and 200 mg/L, at temperature  $30 \pm 0.5$  °C on optimum condition: AC amount 0.4 g/50 mL, agitation speed 400 rpm, contact time 6 min and pH=1.0.

Fig. 8. shows the Tempkin ( $q_e$  vs.  $\ln C_e$ ) plots for adsorption of Mu at  $30 \pm 0.5$  °C temperatures. The constants obtained for Tempkin isotherm are shown in Table 3. The linear form of Dubinin-Radushkevich isotherm equation can be expressed as [52]

$$\ln q_e = \ln Q_m - k\varepsilon^2 \tag{14}$$

where  $Q_m$  is the theoretical monolayer saturation capacity (mg/g),  $k$  is the Dubinin-Radushkevich model constant ( $\text{mol}^2 \text{kJ}^{-2}$ ).  $\varepsilon$ , is the polanyi potential and is equal to

$$\varepsilon = RT \ln \left[ 1 + \frac{1}{C_e} \right] \quad (15)$$

The mean energy of adsorption,  $E$  ( $\text{kJ mol}^{-1}$ ), is related to  $B$  as [53]

$$E = \frac{1}{\sqrt{2k}} \quad (16)$$

The plot of  $\ln q_e$  vs.  $\varepsilon^2$  at different temperatures for Mu is presented in Fig. 8. The constant obtained for D–R isotherms are shown in Table 3. The mean adsorption energy ( $E$ ) gives information about chemical and physical nature of adsorption [54].

The Harkins–Jura adsorption isotherm can be expressed as [55]:

$$\frac{1}{q_e^2} = \left( \frac{B_2}{A} \right) - \left( \frac{1}{A} \right) \text{Log} C_e \quad (17)$$

where  $B_2$  and  $A$  are the isotherm constants. The Harkins–Jura adsorption isotherm accounts to Multilayer adsorption and can be explained with the existence of a heterogeneous pore distribution.  $1/q_e^2$  was plotted vs.  $\log C_e$  (Fig. 8). Isotherm constants and correlation coefficients are summarized in Table 3.

### 3.7. Error analysis

In the single-component isotherm studies, the optimization procedure requires an error function to be defined in order to be able to evaluate the fit of the isotherm to the experimental equilibrium data. However, the use of  $R^2$  is limited to solve linear forms of isotherm equation, but not the errors in isotherm curves. In this study, a Chi-square test was used. The Chi-square test statistic is basically the sum of the squares of the differences between the experimental data and data obtained by calculation from models, with each squared difference divided by the corresponding data obtained by calculation from models [56]. The equivalent mathematical statement is:

$$\chi^2 = \sum_{i=1}^m \frac{(q_{e,\text{exp}} - q_{e,\text{calc}})^2}{q_{e,\text{exp}}} \quad (18)$$

where  $q_{e,\text{exp}}$  is experimental data of the equilibrium capacity (mg/g),  $q_{e,\text{calc}}$  is the equilibrium capacity obtained by calculating from the model (mg/g). If the data from the model are similar to the experimental data,  $\chi^2$  will be a small number, if they are different,  $\chi^2$  will be a large number. Therefore, it is necessary to analyze the data set using Chi-square test to confirm the best-fit isotherm for the adsorption of Mu on AC. The values of  $\chi^2$  for all isotherms at different temperatures were presented in Table 3. By comparing the values of  $\chi^2$  for different isotherms, it was found that Langmuir and Temkin models best-fit the adsorption of Mu on AC.

## 3.8. Thermodynamics parameters

Thermodynamic parameters were evaluated to confirm the adsorption nature of the present study. The thermodynamic constants of the adsorption systems such as change in Gibb's free energy ( $\Delta G^\circ$ ), change in entropy ( $\Delta S^\circ$ ), change in enthalpy ( $\Delta H^\circ$ ), activation energy ( $E_a$ ), and sticking probability ( $S^*$ ) were calculated to evaluate the thermodynamic feasibility and spontaneous nature of the process. Therefore, the thermodynamic constants can be obtained from the following equations:

$$\Delta G^\circ = -RT \ln K_c \quad (19)$$

$$\Delta S^\circ = \Delta H^\circ - \frac{\Delta G^\circ}{T} \quad (20)$$

where  $\Delta G^\circ$  is the free energy change (kJ/mol),  $R$  is the universal gas constant (8.314 J/mol K<sup>-1</sup>),  $K_c$  the thermodynamic equilibrium constant and  $T$  is the absolute temperature (K). Values of  $K_c$  may be calculated from the relation  $\ln q_e/C_e$  vs.  $q_e$  at different temperatures and extrapolating to zero [57, 58]. The thermodynamic parameters are listed in Table 4.  $\Delta S^\circ$  can be used to describe the randomness at the solid-solution interface during the removal process.

**Table 4**

Thermodynamic parameters.

Initial concentration (mg L <sup>-1</sup> )	Parameters	Temperature (K)					
		283.15	293.15	303.15	313.15	323.15	333.15
50	K <sub>c</sub>	8.63	8.42	12.54	14.87	15.56	13.54
		4.00	7.37	9.83	14.50	15.18	18.11
100	$\Delta G^\circ$ (kJ/mol)	-5.07	-5.19	-6.37	-7.03	07.37	-7.39
		-3.26	-4.87	-5.76	-6.96	-7.31	-8.02
Initial concentration (mg L <sup>-1</sup> )	$\Delta S^\circ$ (J/mol K)	$\Delta H^\circ$ (kJ/mol)		$E_a$ (kJ/mol)		$S^*$	
50	58.89	11.67		9.02		2.21×10 <sup>-3</sup>	
100	79.36	18.27		16.79		1.16×10 <sup>-4</sup>	

Positive values of entropy change and enthalpy show increased randomness and endothermic nature of the process respectively, whereas the negative values of free energy confirm the spontaneous nature and feasibility of the adsorption process. The  $\Delta G^\circ$  values were decreased as the temperature was increased from 283.15 to 333.15 K, which is an indication of the physical adsorption nature of the process. The values of other parameters such as enthalpy change ( $\Delta H^\circ$ ), and entropy change ( $\Delta S^\circ$ ), may be determined from Van't Hoff equation

$$\ln K_c = \frac{\Delta H^\circ}{RT} + \frac{\Delta S^\circ}{R} \quad (21)$$

$\Delta H^\circ$  and  $\Delta G^\circ$  can be obtained from the slope and intercept of Van't Hoff plot of  $\ln K_c$  vs.  $1/T$ . The data are presented in Fig. 9 and Table 4.

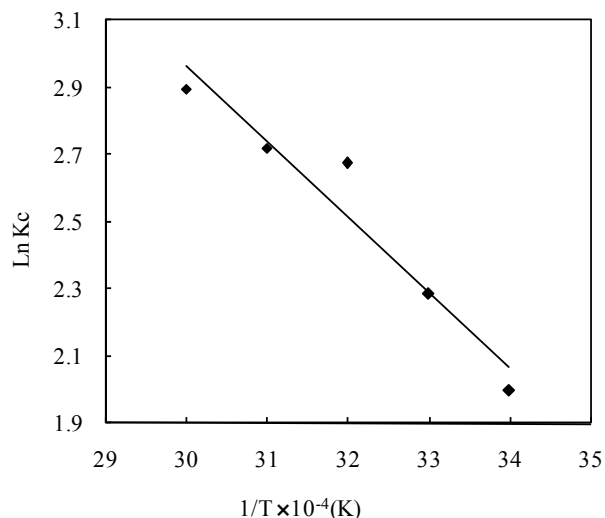


**Fig. 9.** Van't Hoff plots for the adsorption of Mu (100 mg/L) onto AC for evaluating thermodynamic parameters.

The positive values of  $\Delta H^\circ$  further confirm the endothermic nature of the adsorption process and the positive  $\Delta S^\circ$  values suggest the increase in adsorbate concentration in solid-liquid interface indicating thereby the increase in adsorbate concentration onto the solid phase. It also confirms the increased randomness at the solid-liquid interface during adsorption. This is the normal consequence of the physical adsorption phenomenon, which takes place through electrostatic interactions. In order to further support the assertion that physical adsorption is the predominant mechanism, the values of activation energy ( $E_a$ ) and sticking probability ( $S^*$ ) were estimated from the experimental data.

They were calculated using modified Arrhenius type equation related to surface coverage ( $\theta$ ) as follows [36, 58].

$$S^* = (1-\theta)e^{-\frac{E_a}{RT}} \quad (22)$$

The sticking probability,  $S^*$ , is a function of the adsorbate/adsorbent system under investigation, its value lies in the range  $0 < S^* < 1$  and is dependent on the temperature of the system. The parameter  $S^*$  indicates the measure of the potential of an adsorbate to remain on the adsorbent indefinite. The surface coverage  $\theta$  can be calculated from the following equation:

$$\theta = \left[ 1 - \frac{C_e}{C_o} \right] \quad (23)$$

The activation energy and sticking probability were estimated from a plot of  $\ln(1-\theta)$  vs.  $1/T$  (Fig. 10). The positive values of  $E_a$  indicate the endothermic nature of the adsorption process. Table 4 indicates that the probability of MU ions to stick on surface of activated carbon is very high as  $S^* \ll 1$  (Table 4) these values of  $E_a$  and  $S^*$  confirm that, the adsorption process is physisorption.

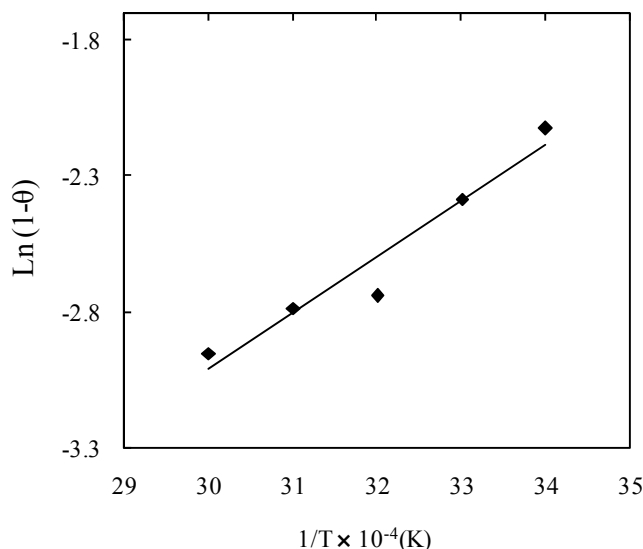


**Fig. 10.** Plots of  $\ln(1-\theta)$  versus  $1/T$  for the adsorption of Mu (100 mg/L) onto AC for evaluating coating constant and activation energy.

#### 4. Conclusion

The present investigation showed that is an effective adsorbent for removal Mu from aqueous solution. The amount of Mu adsorbed was found to vary with initial solution pH, initial Mu concentrations, contact time, and adsorbent dose. Removal of Mu is pH dependent and the maximum removal was attained at pH=1.0. The equilibrium adsorption is practically achieved in 6 minutes. It was also a function of adsorbate concentration and temperature of the solution. The adsorption-desorption study showed that the adsorption was reversible and followed the ion-exchange mechanism. Adsorption equilibrium data follows Langmuir, Freundlich, Tempkin, Dubinin-Radushkevich and Harkins-Jura isotherm models. The equilibrium data fitted very well in a Langmuir and Tempkin isotherm equations. The kinetic study of Mu onto AC was performed based on pseudo-first-order, pseudo-second-order, Elovich and intra-particle diffusion equations. The data indicate that the adsorption kinetics follow the pseudo-second-order rate with intra-particle diffusion as one of the rate determining steps. The determination of the thermodynamic parameters ( $\Delta G^\circ$ ,  $\Delta H^\circ$ ,  $\Delta S^\circ$ ,  $E_a$  and  $S^*$ ) indicates the spontaneous and endothermic nature of the adsorption process. The positive sign of  $\Delta S^\circ$  indicates that the adsorption process takes place through electrostatic interaction between adsorbent surface and adsorbate species in solution. The activation energy of adsorption of Mu was found to be 9.02 and 16.79 kJ/mol indicating that the adsorption process is endothermic with a physical nature. The present study concludes that the AC could be employed as low-cost adsorbents for the removal of Mu from aqueous solution in general.

#### References

- [1] R. O. A. de Lima, A. P. Bazo, D. M. F. Salvadori, C. M. Rech, D. P. Oliveira, G. A. Umbuzeiro, *Mutat. Res.* 626 (2007) 53-60.
- [2] M. S. Tsuboy, J. P. F. Angeli, M. S. Mantovani, S. Knasmüller, G. A. Umbuzeiro, L. R. Ribeiro, *Toxicol. In Vitro* 21 (2007) 1650-1655.
- [3] R. Caritá, M. A. Marin-Morales, *Chemosphere* 72 (2008) 722-725.
- [4] F. A. Pavan, S. L. P. Dias, E. C. Lima, E. V. Benvenuti, *Dyes Pigm.* 76 (2008) 64-69.
- [5] F. A. Pavan, Y. Gushikem, A. S. Mazzocato, S. L. P. Dias, E. C. Lima, *Dyes Pigm.* 72 (2007) 256-266.
- [6] V. A. Shenai, *Colourage*, 43 (1996) 41-46.
- [7] J. C. Greene, G.L. Baughman, *Text. Chem. Color.* 28 (1996) 23-26.

- [8]. F. A. Pavan, E. C. Lima, S. L. P. Dias, A. C. Mazzocato, *J. Hazard. Mater.* 150 (2008) 703-712.
- [9] M. Shamsipur, N. Alizadeh, *Talanta*, 39 (1992) 1209-1212.
- [10] Y. Akhlaghi, M. K. Zarch, *Anal. Chim. Acta*, 537 (2005) 331-338.
- [11] K. Santhy, P. Selvapathy, *Bioresour. Technol.* 97 (2006) 1329-1336.
- [12] M. N. Khan, A. Sarwar, U. Zareen, Fahimuddin, *Pak. J. Anal. Chem.* 3 (2002) 8-12.
- [13] G. Mckay, J. F. Porter, G. R. Prasad, *Water Air Soil Pollut.* 114 (1999) 423-438.
- [14] M. Dogan, M. Alkan, Y. Onganer, *Water Air Soil Pollut.* 120 (2000) 229-248.
- [15] O. Demirbas, M. Dogan, *Adsorption* 8 (2002) 341-349.
- [16] M. Dogan, M. Alkan, *J. Colloid Interf. Sci.* 267 (2003) 32-41.
- [17] M. Dogan, M. Alkan, *Chemosphere* 50 (2003) 517-528.
- [18] M. Dogan, M. Alkan, *Fresenius Environ. Bull.* 12 (2003) 418-425.
- [19] M. Alkan, M. Dogan, *J. Colloid Interf. Sci.* 243 (2001) 280-291.
- [20] G. Bereket, A. Z. Arogus, M. Z. Ozel, *J. Colloid Interf. Sci.* 187 (1997) 338-343.
- [21] M. M. Mohamed, *Physicochem. Eng. Aspects* 108 (1996) 39-48.
- [22] D. Mohan, K. P. Singh, K. Kumar, *Ind. Eng. Chem. Res.* 42 (2002) 1965-1976.
- [23] S. J. Allen, G. Mckay, K. Y. H. Khader, *J. Chem. Technol. Biotechnol.* 45 (1989) 291-302.
- [24] Y. S. Ho, G. Mckay, *Chem. Eng. J.* 70 (1998) 115-124.
- [25] G. Mckay, M. S. Otterburn, A. G. Sweeney, *Water Res.* 15 (1981) 327-331.
- [26] E. Demirbas, M. Kobya, M. T. Sulak, *Bioresour. Technol.* 99 (2008) 5368-5373.
- [27] D. Kavitha, C. Namasivayam, *J. Chem. Eng.* 139 (2008) 453-461.
- [28] M. J. Iqbal, M. N. Ashiq, *J. Hazard. Mater.* 139 (2007) 57-66.
- [29] D. Kavitha, C. Namasivayam, *Chem. Eng. J.* 139 (2008) 453-461.
- [30] K. Ravikumar, B. Deebika, K. Balu, *J. Hazard. Mater.* 122 (2005) 75-83.
- [31] M. Strest, D. Naden, *Ion exchange and sorption process in hydrometallurgy chapter 2*, 1987.
- [32] J. Acharya, J. N. Sahu, B. K. Sahoo, C. R. Mohanty, B. C. Meikap, *J. Chem. Eng.* 150 (2009) 25-39.
- [33] F. Suarez-Garcia, A. Martinez-Alonso, J. M. D. Tascon, *Carbon* 42 (2004) 1419-1426.
- [34] M. Ghaedi, M. K. Amini, A. Rafi, S. Gharaghani, A. Shokrollahi, *Ann. chim.* 96 (2005) 457-464.
- [35] A. Shokrollahi, M. Ghaedi, H. Ghaedi, *J. Chin. Chem. Soc.* 54 (2007) 933-940.
- [36] F. A. Pavan, E. C. Lima, S. L. P. Dias, A. C. Mazzocato, *J. Hazard. Mater.* 150 (2008) 703-712.
- [37] J. C. P. Vaghetti, E. C. Lima, B. Royer, J. L. Brasil, B. M. da Cunha, N. M. Simon, N. F. Cardoso, C. P. Z. Noreña, *J. Biochem. Eng.* 42 (2008) 67-76.
- [38] B. Guo, L. Hong, H. X. Jiang, *Ind. Eng. Chem. Res.* 42 (2003) 5559-5567.
- [39] P. Chingombe, B. Saha, R. J. Wakeman, *J. Colloid Interf. Sci.* 302 (2006) 408-416.
- [40] S. Lagergren, *Zur theorie der sogenannten adsorption geloster stoffe*, *Kunliga. Svenska vetenskademien. Handlingar.*, 24 (1898) 1-39.
- [41] A. A. Ahmed, B. H. Hameed, N. Aziz, *J. Hazard. Mat.* 141 (2007) 70-76.
- [42] G. Mckay, Y.S. Ho, *Process Biochem.* 34 (1999) 451-465.
- [43] S. H. Chien, W. R. Clayton, *J. Soil Sci. Am.* 44 (1980) 265-268.
- [44] W. J. Weber, J. C. Morris, *J. Santi. Eng. Div. Am. Soc. Civil Eng.* 89 (1963) 31-59.
- [45] D. I. Mall, V. C. Srivastava, N. K. Agarwal, *Dyes Pigm.* 69 (2006) 210-223.
- [46] I. Langmuir, *J. Am. Chem. Soc.* 40 (1918) 1361-1403.
- [47] I. Langmuir, *J. Am. Chem. Soc.* 38 (1916) 2221-2295.
- [48] O. Abdelwahab, *Desalin.* 222 (2008) 357-367.
- [49] N. Chilton, J. N. Losso, W. E. Marshall, *Bioresour. Technol.* 85 (2002) 131-135.
- [50] H. M. F. Freundlich, *Phys. Chem. (Leipzig)* 57A (1906) 385-470.
- [51] M. J. Temkin, V. Pyzhev, *Acta Physiochim. USSR* 12 (1940) 217-222.
- [52] M. M. Dubinin, L.V. Radushkevich, *Chem. Zentr.* 1 (1947) 875.
- [53] M. M. Dubinin, *Chem. Rev.* 60 (1960) 235-266.
- [54] W. Rieman, H. Walton, *Ion exchange in analytical chemistry International Series of Monographs in Analytical Chemistry*, vol. 38, Pergamon Press, Oxford, 1970.
- [55] C. A. Basar, *J. Hazard. Mater. B* 135 (2006) 232-241.
- [56] N. K. Amin, *J. Hazard. Mater.* 165 (2009) 52-62.
- [57] A. A. Khan, R. P. Singh, *J. Colloid Sci.* 24 (1987) 33-42.
- [58] M. H. Jnr, A. I. Spiff, *J. Biotechnol.* 8 (2005) 162-169.